LAWRENCE
LIVERMORE
NATIONAL
LABORATORY

UCRL-JRNL-206120

Thermoelastic Effects as a Way of Creating Transient Renewable Reflective Optics

D. D. Ryutov

August 18, 2004

Review of Scientific Instruments

Thermoelastic effects as a way of creating transient renewable reflective optics

D.D. Ryutov

Lawrence Livermore National Laboratory, Livermore, CA 94551

Abstract

A technique for creating renewable reflective optics suitable for focusing of pulsed laser beams is proposed. It is based on the heating of the surface of a planar reflecting slab by an auxiliary heating source that causes thermal expansion of the slab material and creates a desired surface relief. The presence of this relief is a transient phenomenon, but, for short-enough main pulse, this does not cause any problems. If the surface is damaged by the main pulse, the shifting of the slab and repeating the whole cycle allows recreating the transient mirror. Favorable features of this approach include controlling the optics "at a distance", without any direct mechanical contact. Detailed discussion of the possibilities provided by this technique for the focusing of x-ray beams at the planned LCLS facility at Stanford is presented. It is concluded that 10-fold increase of intensity of 8-keV beam and 100-fold increase of intensity of 0.8 keV beam is possible. A set of design equations and constraint is formulated. The analysis presented can be used as a template for analyses of similar transient optical systems for the UV and optical range.

Basic notation

A_a – albedo with respect to the auxiliary pulse

A_x - albedo with respect to the x-ray pulse

C – the ratio of the initial beam radius to the beam radius at the focal plane (r_F/r)

E – Young's modulus

F – focal length of the mirror

G – yield strength

I – energy flux during the auxiliary pulse

N – intensity enhancement factor for the x-ray beam (energy flux in the focal plane/ initial energy flux)

$<P>$ - average power of the auxiliary heating system

Q – energy absorbed per unit area during the auxiliary pulse

S- safety factor (yield strength/maximum stress)

T – temperature of the material

W – energy per pulse delivered by the auxiliary laser

a – thickness of the reflecting slab

c_p – specific heat

f – the ratio of the focal length to the beam diameter

h – normal displacement of the surface caused by thermal expansion at the end of the auxiliary pulse

k – wave-number of the spatial Fourier transform

l – length-scale of the surface perturbations

$q(t)$ – function that determines the pulse shape for the auxiliary laser

r - initial beam radius

r_F – beam radius in the focal plane

t_a – duration of the auxiliary heating pulse

t_x- time between two successive x-ray pulses ($1/t_x$ - repetition rate)

u_i – displacement vector

u_{ik} – strain tensor

v - tangential velocity of the mirror

α - volumetric thermal expansion coefficient

$\delta\varphi$ – deviation of the tilt of the surface from the one corresponding to the perfect shape

θ – grazing incidence angle

μ – Poisson ratio

$\rho_{\|}$, $\rho_{\perp}$ - curvature radii of the mirror in the parallel and perpendicular direction (with respect to the beam axis)

σ_{ik} – stress tensor

χ – thermal diffusivity

ψ – a scalar function related to the stress tensor (Eq. (10))

I. INTRODUCTION

This paper is concerned with a concept of renewable optics for ultra-high-intensity, pulsed, rep-rate x-ray beams to be produced at the Linac Coherent Light Source (LCLS), planned at Stanford Linear Accelerator Center. LCLS is the 4th generation free electron laser [1] and its characteristic feature is an extremely high brightness of x-ray beams. Parameters of the beams for two typical modes of operation of LCLS are presented in Table I. A similar facility is planned in Germany [2].

A broad variety of proposed experiments [3] require further manipulation of the LCLS beam, in particular, its deflection and focusing/defocusing. This can be achieved by using a grazing-incidence reflective optics [4]. In order to have a high-enough reflectivity in the x-ray range, the angle of incidence will have to be as low as a few milliradians (see Table II based on Ref. 5).

Despite a small incidence angle, the fluence remains quite high, raising a concern of a possible damage to the optics. The damage can be caused by a variety of effects (e.g., [6-9], and references therein) and may occur anywhere between one pulse and a few thousands of pulses (at the designed repetition rate of 120 Hz one thousand of pulses means only 8 seconds of operation). A possible way of solving this problem is to use renewable optical elements. Earlier, a possibility of using liquid renewable optics has been analyzed [10, 11]. Here we propose a simpler and less expensive approach.

The general geometry of the problem is illustrated on Fig. 1, where a planar polished reflecting slab is shown and the coordinate frame that will be used throughout this report is introduced.

The basic idea of our approach is illustrated by Fig. 2. We start from a planar slab of a reflecting material. Assume that we irradiate the initial flat surface of the slab by an auxiliary laser pulse, at an angle not much different from the normal, and wavelength corresponding to as strong surface absorption as possible. This could be a visible or UV radiation. The role of this auxiliary laser is to heat the surface of the slab in a desired surface pattern. Then, the thermal expansion will create a desired surface relief, say, a focusing or defocusing mirror. Shown in Fig.2 is a relief corresponding to a focusing elliptic mirror. After the passage of the main pulse, the surface may be damaged and become unusable for the next shot. The flat metal plate would then be shifted tangentially by a sufficient distance to expose a fresh surface element. The auxiliary laser would be fired again, creating a desired surface relief, main pulse would arrive, etc. As we show below, the power needed from the auxiliary laser is quite small, so that the optics of this auxiliary laser will survive the whole experimental campaign. This general approach can be called the TEL optics (Thermo-ELastic optics).

The "fresh" surface in a high repetition-rate facility of the type of LCLS can be provided by, for example, rotating a polished disc, as shown in Fig. 3a, or a polished cylinder, as shown on Fig. 3b (in the latter case, the curvature of the cylinder must be much smaller than the curvature of the optic created on its surface). The disc will also slowly move in the direction shown by a block arrow, so that eventually all the disc surface would be used. For the same purpose, the cylinder would be slowly moved along the axis. As the size of the mirrors in the case of LCLS is less than a millimeter across, one can produce tens of thousands of reflections before the whole surface of the disc or the cylinder is covered. If a certain surface element can be used, say, 1000 times before a

significant damage occurs, the cylinder (or disc) would survive a few hours of a continuous LCLS operation.

A natural question arises as to whether this approach is better than just pre-manufacturing tens of thousands of miniature mirrors on the surface of the disc or a cylinder. We believe that doing the latter with a sufficient accuracy will involve very large costs, whereas creating just a polished disc or cylinder without any imprinted 3D structures is a much simpler task. The only additional element required by the TEL optics is an auxiliary heating system, but its parameters, as we show in Sec.IX are rather trivial, and it will survive the whole experimental campaign (months and years).

One more advantage of the TEL optics is that one can change its parameters very rapidly, even on the pulse-to-pulse basis, just by changing the illumination pattern of the reflecting surface.

To be specific, we consider creating in this fashion a mirror which would focus a parallel incident beam at a distance F from the center of the mirror (Fig. 2). The shape of the reflecting surface (for the incidence angle $\theta<<1$) should then be as follows:

$$-x = \frac{\theta}{4F} z^2 + \frac{1}{4F\theta} y^2. \qquad (1)$$

The level lines x=const are nested ellipses. The parameter $d=OB$ (unimportant in terms of optical properties of the mirror) is the distance from the center of the mirror to the unperturbed surface of the slab. The shape (1) is not absolutely perfect in terms of aberrations; one may want to add higher-order corrections in y and z to the r.h.s. to eliminate aberrations. This shape adjustment is certainly possible within the TEL approach but we will not discuss it in this initial paper.

As usual with the x-ray optics, we measure the incidence angle θ from the plane of the mirror (not from the normal to the mirror). Throughout this paper we heavily exploit the condition $\theta << 1$ The need to work with very shallow incidence angles, as low as 3 mrad in the case of a 8-keV beam, makes the use of reflective optics very challenging. On the other hand, use of the multilayers or transmission zone plates is limited by the damage to these expensive optics that may occur, at full beam parameters, within a limited number of pulses. Also, transmission optics is hardly feasible at the lower end of the LCLS energies (less than 2 keV), because of very short absorption lengths for the corresponding quanta.

We concentrate on a quantitative analysis of the shapes of the surfaces attainable within the TEL approach. We do not discuss issues of the integrated design which will be addressed in subsequent publications.

A key problem here is that the non-uniform heating creates thermal stresses in the mirror. The higher the curvature of the mirror surface, the shorter the focal length (which is desirable); on the other hand, the higher the curvature, the higher the stresses, the higher risk of a permanent damage to the optics. One has to find a reasonable compromise between these two trends.

Although the primary motivation for this work was an analysis of the reflective optics for LCLS, other applications are also possible, in particular, for creating reflecting optics whose parameters could be "dialed in" within 0.01-1 ms prior to the arrival of the main pulse. In this context, the proposed concept of TEL optics could be applied not only to x rays but also to the visible and UV range (with an obvious caveat that diffraction limitations have to be observed, and the reflectivity has to be sufficient). For these longer

wavelengths, the incidence angle can be made substantially larger than mentioned in Table II, and implementation of the concept becomes simpler.

This paper is organized as follows: In Sec. II, we present basic equations for the thermo-elastic equilibrium. We note that, because of a strongly elongated heating pattern, the problem is effectively two-dimensional. In Sec. III we present an analytic solution of this problem and obtain a criterion on allowable temperature increase (the one at which the thermal stress does not exceed the yield strength). In Sec. IV, we consider constraints on the temporal parameters of the heating pulse and present an optimum pulse shape. In Sec. V, we obtain a convenient expression for the focal length of the mirror compatible with lower-than-yield-strength stresses. This is one of the main results of our paper. In Sec. VI, we discuss numerical values of the heating times. We find these times to be much longer than the times required for establishing mechanical equilibrium; this justifies the static approach to the elasticity problem. In Sec. VII, we consider complications associated with imperfections of the auxiliary laser intensity distribution and imperfections of the material properties. Sec. VIII deals with diffraction limitations. In Sec. IX the energy per auxiliary pulse and the average power of the auxiliary heating system are evaluated. In Sec X we evaluate the velocity at which the reflecting surface should be moved in the tangential direction. Sec. XI briefly discusses possible variations of the basic concept. Finally, Sec. XII contains discussion of the results obtained.

What we present here is a broad scoping study; the “fine tuning” is left for the future work.

II. BASIC EQUATIONS

We will be using standard equations of the linear elasticity theory, which can be found, e.g., in Ref. [12]. Although these equations and the way of solving them are well known, there is a number of specific issues related to the problem of the TEL optics which had not been addressed thus far.

The stress-strain relation is [12]:

$$\sigma_{ik} = -\frac{E\alpha\delta T}{3(1-2\mu)}\delta_{ik} + \frac{E}{1+\mu}\left(u_{ik} + \frac{\mu}{1-2\mu}u_{ll}\delta_{ik}\right) \tag{2}$$

where σ_{ik} and u_{ik} are the stress and strain tensors, respectively, E is Young's modulus, μ is the Poisson ratio, α is the volumetric thermal expansion coefficient, and δT is a temperature variation with respect to the initial uniform temperature. The strain tensor is related to the deformation vector $\boldsymbol{u}$ by the equation

$$u_{ik} = \frac{1}{2}\left(\frac{\partial u_i}{\partial x_k} + \frac{\partial u_k}{\partial x_i}\right) \tag{3}$$

The equations of the mechanical equilibrium of the medium are:

$$\frac{\partial \sigma_{ik}}{\partial x_k} = 0 \tag{4}$$

For a beam of a circular cross-section, the beam imprint at a grazing incidence will be a long ellipse (Fig. 1). The surface relief, as well as the temperature distribution required to create it, will also be of a similar structure. This means that, at every particular value of the coordinate z, we can consider a 2D equilibrium, where the stresses and deformations depend only on the coordinates x and y, whereas the coordinate z enters the problem just as a parameter. In other words, we can solve a 2D problem instead of a 3D problem. The orientation of the coordinate axes is shown on Fig. 1.

In this 2D problem, only three components of the strain tensor will be non-zero: u_{xx}, $u_{xy}(=u_{yx})$, and u_{yy}. Components of the stress tensor that enter the equilibrium equation are σ_{xx}, $\sigma_{xy}(=\sigma_{yx})$, and σ_{yy} (generally speaking, there exists also the σ_{zz} component [12] but it does not enter the equilibrium condition). In the 2D problem one has:

$$\sigma_{xx} = -\frac{\alpha E \delta T}{3(1-2\mu)} + \frac{(1-\mu)E}{(1-2\mu)(1+\mu)} u_{xx} + \frac{\mu E}{(1-2\mu)(1+\mu)} u_{yy} \tag{5}$$

$$\sigma_{xy} = \frac{E}{1+\mu} u_{xy} \tag{6}$$

$$\sigma_{yy} = -\frac{\alpha E \delta T}{3(1-2\mu)} + \frac{(1-\mu)E}{(1-2\mu)(1+\mu)} u_{yy} + \frac{\mu E}{(1-2\mu)(1+\mu)} u_{xx} \tag{7}$$

$$\sigma_{zz} = -\frac{\alpha E \delta T}{3(1-2\mu)} + \frac{\mu E}{(1-2\mu)(1+\mu)} (u_{xx} + u_{yy}) \tag{8}$$

The equilibrium conditions (4) reduce to

$$\frac{\partial \sigma_{xx}}{\partial x} + \frac{\partial \sigma_{xy}}{\partial y} = 0; \;\; \frac{\partial \sigma_{yx}}{\partial x} + \frac{\partial \sigma_{yy}}{\partial y} = 0. \tag{9}$$

As pointed out in [12], the solution to these equations can be expressed in terms of a single auxiliary scalar function ψ such that

$$\sigma_{xx} = \frac{\partial^2 \psi}{\partial y^2}, \;\; \sigma_{xy} = -\frac{\partial^2 \psi}{\partial x \partial y}, \;\; \sigma_{yy} = \frac{\partial^2 \psi}{\partial x^2}, \tag{10}$$

so that the equilibrium conditions (9) are satisfied identically. Following Ref. [12], we note that, by summing Eqs. (5) and (7), one obtains that

$$\sigma_{xx} + \sigma_{yy} = \nabla^2 \psi = -\frac{2\alpha E \delta T}{3(1-2\mu)} + \frac{E}{(1-2\mu)(1+\mu)} (u_{xx} + u_{yy}). \tag{11}$$

On the other hand, by taking the divergence of Eq. (7.8) of Ref. [12], one finds that

$$\nabla^2 (u_{xx} + u_{yy}) = \frac{(1+\mu)\alpha}{3(1-\mu)} \nabla^2 \delta T. \tag{12}$$

Then, applying an operator ∇^2 to Eq. (11) one finds an equation which is the basis for the further analysis:

$$\nabla^2(\nabla^2\psi) = -\frac{\alpha E}{3(1-\mu)}\nabla^2\delta T\,. \tag{13}$$

This equation coincides with equation (3) of Ref. [7].

The boundary conditions at the free surface (x=0) are:

$$\sigma_{xx} = 0;\ \ \sigma_{xy} = 0 \tag{14}$$

At $x \to \infty$ the stresses and strains vanish.

For a given temperature distribution, by solving equation (13), one finds χ and, by virtue of Eq. (10), the stresses; then, by using Eqs. (5)-(8), one finds the strains and the deformation vector.

III. DEFORMATION OF THE SURFACE

A. General case

To solve the problem, we use the Fourier decomposition of functions χ and δT over the coordinate y,

$$\psi_k = \frac{1}{\sqrt{2\pi}}\int_{-\infty}^{+\infty}\psi e^{-iky}dy;\ \ \Delta T_k = \frac{1}{\sqrt{2\pi}}\int_{-\infty}^{+\infty}\Delta T e^{-iky}dy\,. \tag{15}$$

A Fourier-transformed equation (13) acquires the form:

$$\left(\frac{d^2}{dx^2} - k^2\right)\cdot\left[\frac{d^2\psi_k}{dx^2} - k^2\psi_k + \frac{\alpha E}{3(1-\mu)}\delta T_k\right] = 0\,. \tag{16}$$

The boundary conditions (14), expressed in terms of ψ_k, are:

$$\psi_k\Big|_{x=0} = 0;\ \ \frac{d\psi_k}{dx}\Big|_{x=0} = 0\,. \tag{17}$$

From Eq. (16) we conclude that

$$\frac{d^2\psi_k}{dx^2} - k^2\psi_k + \frac{\alpha E}{3(1-\mu)}\delta T_k = C_1 e^{-|k|x}, \tag{18}$$

where C_1 is some constant, and we have not included the exponentially growing term in the right-hand side. The solution of this equation, vanishing at $x\to\infty$, is:

$$\psi_k = -\frac{C_1 x e^{-|k|x}}{2|k|} + C_2 e^{-|k|x} + \frac{\alpha E}{6(1-\mu)|k|}\left[e^{|k|x}\int_x^\infty e^{-|k|x'}\delta T_k dx' + e^{-|k|x}\int_0^x e^{|k|x'}\delta T_k dx'\right] \tag{19}$$

The constants C_1 and C_2 can be found from the boundary conditions (17):

$$C_1 = \frac{2\alpha E|k|}{3(1-\mu)}\int_0^\infty \delta T_k e^{-|k|x'}dx';\;\; C_2 = -\frac{\alpha E}{6(1-\mu)|k|}\int_0^\infty \delta T_k e^{-|k|x'}dx' \tag{20}$$

This solves the problem of the stresses generated in the slab. For a specific dependence of the temperature vs the x-coordinate, ~exp(-qx), integration in (19) yields Eq. (9) of Ref. [7].

A useful relation can be obtained from Eq. (18) by integrating it from zero to infinity, and imposing the second of the boundary conditions (14). The result is:

$$\int_0^\infty \sigma_{xxk}dx' \equiv -k^2\int_0^\infty \psi_k dx' = \frac{C_1}{|k|} - \frac{\alpha E}{3(1-\mu)}\int_0^\infty \delta T_k e^{-|k|x'}dx' = \frac{\alpha E}{3(1-\mu)}\int_0^\infty \delta T_k e^{-|k|x'}dx' \tag{21}$$

Now we are prepared to find the deformation of the surface. Eliminating u_{yy} from Eqs. (5) and (7), we find:

$$\frac{\partial u_{xk}}{\partial x} = u_{xxk} = \frac{\alpha\delta T_k(1+\mu)}{3} + \sigma_{xxk}\frac{1-\mu^2}{E} - \sigma_{yyk}\frac{\mu(1-\mu)}{E} \tag{22}$$

Integrating this equation from zero to infinity, using Eq. (21), and taking into account that

$$\int_0^\infty \sigma_{yyk}dx = \int_0^\infty \frac{d^2\psi_k}{dx^2}dx = -\frac{d\psi_k}{dx}\Big|_{x=0} = 0 \tag{23}$$

we find:

$$-u_{xk}\big|_{x=0} = \frac{\alpha(1+\mu)}{3}\int_0^\infty \left(1+e^{-|k|x}\right)\delta T_k dx \tag{24}$$

The remarkably simple Eq. (24) is the basis of our further analysis of the deformations of the surface.

In the analysis of the optical part of the problem, instead of u_x, we use the notation

$$h(y,z) \equiv -u_x(x=0,y,z); \tag{25}$$

h(y,z) is the height of the surface relief over the unperturbed surface (this is more convenient, because, for the direction of the axis *x* assumed in our paper, u_x is negative when the surface is heated up).

B. Special case of a thin heated layer

Of a particular interest is the case where the thickness of the heated layer is small compared to the beam radius (short-enough heating pulses). Otherwise, the tangential redistribution of heat makes impossible the control over the structures with the width of order of the beam radius. For the case of a thin heated layer, the analysis is particularly straightforward as the characteristic wave-number *k* of the Fourier decomposition of δT satisfies condition $kx<<1$. Then, replacing $\exp(-|k|x)$ in Eq. (24) by unity and performing the inverse Fourier transform, one obtains:

$$h(y,z) = \frac{2\alpha(1+\mu)}{3}\int_0^\infty \delta T(x,y,z)dx = \frac{2\alpha(1+\mu)}{3c_P}Q(y,z) \tag{26}$$

where *h* is defined by Eq. (25), c_p is specific heat, and *Q* is the absorbed energy per unit area of the mirror. We see that the surface displacement is proportional to Q .

We will consider only monotonous temperature distributions in the *z* direction, with the temperature decreasing into the material (in other words, we assume that the heating occurs from the surface). As was shown in Ref. [7], in the case of a thin heated layer, the stress reaches the maximum near the surface, where the *yy* and *zz* components of the stress tensor are dominant. They are:

$$\sigma_{yy}(0,y,z) = \sigma_{zz}(0,y,z) = -\frac{\alpha E}{3(1-\mu)}\delta T(0,y,z) \tag{27}$$

The condition that the yield strength has not been reached reads as a constraint on the maximum admissible temperature increase at the surface (see Eq. (17) in Ref. [7][1]):

$$\frac{\alpha E \delta T}{3(1-\mu)} < G \tag{28}$$

We introduce a "safety factor" $S>1$, which shows by how much we haven't reached the yield strength of the material. In other words, we use the following expression for the maximum surface temperature:

$$\max \delta T = \frac{3(1-\mu)G}{S\alpha E} \tag{29}$$

IV. CREATING THE NECESSARY TEMPERATURE DISTRIBUTION

Temporal dependence of the heating pulse should be chosen in such a way, that, for a given total absorbed energy per unit area, Q, the maximum (over the pulse length) surface temperature be minimum. We denote the pulse length by t_0, and characterize the pulse shape by a dimensionless function $q(t)$ (Fig. 4) such that

$$\int_0^{t_0} q(t)dt = t_0 \tag{30}$$

As shown in Ref. [13], in a 1D heat conduction problem, the surface temperature is related to the function $q(t)$ by the equation:

$$\delta T(t) = \frac{Q}{c_p\sqrt{\pi\chi}}\int_0^t \frac{q(t')dt'}{\sqrt{t-t'}} \tag{31}$$

[1] Note a typo in Ref. 7: the numerical values of the thermal expansion coeffcient α presented in the Table II of that paper correspond to a *linear* expansion coefficient, whereas in all the equations and numerical estimates a *volumetric* expansion coefficient had been used; to fix this inconsistency, one should just multiply the numerical values of α in the aforementioned Table II by a factor of 3, without changing anything else in the paper. In our present paper a Table III contains correct (volumetric) values of α.

where c_p is the specific heat, and χ is the thermal diffusivity. One can show that the best result corresponds to $q \sim t^{-1/2}$. In this case, the surface temperature remains constant during the pulse (Fig. 4), with

$$\delta T(t) = \frac{Q}{c_p}\sqrt{\frac{\pi}{4\chi t_0}} \tag{32}$$

For comparison, Fig. 4 shows also the temperature evolution for the constant *q(t)*. In this case, the temperature grows with time and, at the end of the heating pulse is

$$\delta T(t_0) = \frac{Q}{c_p}\sqrt{\frac{4}{\pi\chi t_0}} \tag{33}$$

One sees that, in the case of the optimum pulse ($q \sim t^{-1/2}$), the surface temperature at the end of the pulse is less than in the case of a flat-top pulse by approximately 30%. Of course, there is a formal singularity in the irradiation power at t=0, which should be somewhat smoothed (Fig. 4). The temperature distribution inside the material at $t=t_0$ for these two cases is shown in Fig. 5.

Increasing the pulse length t_0 at a given total energy Q leads to the decrease of the surface temperature (which is desirable, because of the constraint (28)). The limit on t_0 is set by the effect of the transverse spreading of the heat. If one waits for too long, the features of the scale ~ r are smoothed, and one loses control over the surface relief on the scale r. We will fold the corresponding constraint into our analysis by requiring that the lateral spreading of the heat during the time t_0 does not exceed a half of the beam radius r, i.e.,

$$2\chi t_0 = \left(\frac{r}{2}\right)^2 \tag{34}$$

Together with condition (26), this yields the following expression for the temperature increase:

$$\delta T = \sqrt{2\pi}\,\frac{Q}{rc_p} \tag{35}$$

We assume that the thickness of the slab should exceed by a factor of a few the beam radius, as otherwise the effect of the opposite surface of the slab on the mechanical equilibrium may become important.

V. THE MINIMUM FOCAL LENGTH

According to Eq. (26), the surface relief is determined by the spatial distribution of the absorbed heat, $Q(y,z)$ and, whence, according to Eq. (35), by the temperature distribution. An imprint of the cylindrical beam boundary has a form of an ellipse. The "elevation" over the central point of the mirror at the beam boundary is, according to Eq. (1), $h=r^2/4\theta F$. As the finite thermal diffusivity prevents the temperature profiles from having sharp breaks, the "ridge" surrounding the central "crater" will be higher than $h=r^2/4\theta F$ (Fig. 2b). We assume that the maximum height of the "ridge" is a factor of 2 greater, i.e.,

$$h_{max}=r^2/2\theta F. \tag{36}$$

Using Eqs. (26), (35) and (36), one finds that

$$\delta T_{\max} = \frac{3\sqrt{2\pi}}{4\alpha(1+\mu)}\,\frac{r}{\theta F}. \tag{37}$$

Then, the constraint (29) sets the limit on the shortest possible focal length,

$$F_{\min} = \frac{r}{\theta}\times\frac{\sqrt{2\pi}S}{4(1-\mu^2)}\times\frac{E}{G}. \tag{38}$$

This equation can be considered as the main result of this study: it relates the minimum possible focal length to material constants and geometrical characteristics of the system. The parameter S (safety factor) shows by how much the maximum stress is below the yield strength. The ratio of the focal length to the beam diameter (the f-factor) is, obviously,

$$f = \frac{\sqrt{2\pi}S}{8\theta\left(1-\mu^2\right)} \times \frac{E}{G}. \tag{39}$$

Fig. 6 shows δT_{max} evaluated on the basis of Eqs. (36) and (39) for aluminum and beryllium vs the parameter $f\theta$ for S=1.5. The temperature increase δT_{max} is small compared to the melting temperature. Therefore, there will be no substantial changes in the Young modulus, and one can neglect effects associated with the change of the elastic properties of the material in the course of heating.

The typical f-value evaluated from Eq. (39) is quite large. This may cause the diffraction broadening of the focal spot. We address this issue in Sec. VIII.

The curvature radius ρ of the mirror, within the beam aperture, can be found from Eqs. (1) and (38). One has

$$\rho_{\perp} = \sqrt{\frac{\pi}{2}} \frac{rS}{1-\mu^2} \times \frac{E}{G}, \quad \rho_{\parallel} = \sqrt{\frac{\pi}{2}} \frac{rS}{1-\mu^2} \times \frac{E}{\theta^2 G} \tag{40}$$

where the subscripts $\perp$ and $\parallel$ correspond to the directions across the beam imprint (y, on Fig.1) and along the beam imprint (z, on Fig. 1). One sees that in the “across” direction the curvature radius for the 8-keV beam is a few centimeters. Accordingly, for the orientation of the reflecting cylinder shown on fig. 3b, there will be only minor corrections introduced by the initial curvature of the cylinder if its radius is 20-25 cm.

On the lower end of the x-ray energies, i.e., at 0.8 keV, the energies below a couple of keV, $\rho_\perp$ becomes quite large, in the range of 10 cm. To accommodate such structures on the outer side of the cylinder, as shown on Fig. 3b, would require too large cylinder radii, approaching a meter. On the other hand, one can use in this case a different approach, where reflections would occur from the inner surface of a cylinder, as shown on Fig. 3c. In this case, the thermal deformation of the surface would be superimposed on the already curved surface. One can show that this would allow for shorter focal lengths than for a planar initial surface.

The parallel curvature radius, $\rho_\parallel$, is large, $\rho_\parallel = \rho_\perp / \theta^2$.

VI. CHARACTERISTIC TIMES INVOLVED

As has already been mentioned, the auxiliary pulse length t_0 is limited by the process of the heat spreading across the elliptical mirror, Eq. (34); t_0 determines the time within which a desired optics can be created on a "pristine" surface of the slab. This time is plotted on Fig. 7. It goes without saying, that the main pulse should be at least by the factor of 10 shorter than the auxiliary pulse.

In our analysis, we have assumed that the medium reaches the state of a mechanical equilibrium, i.e. that the acoustic signal has enough time to travel through the slab and back, as well as to travel over the length of the heated zone. This is certainly the case even for relatively slow transverse acoustic waves, see the values of $s_\perp$ in Table III. Note also that, as the heating pulse is so slow, the acoustic waves will actually not be generated, the whole process will be of a character of a sequence of equilibria determined by the instantaneous temperature distribution. Generation of acoustic waves will then be strongly suppresses, meaning that there will be no "rattling" of the surface after the pulse.

VII. THE ROLE OF IMPERFECTIONS OF THE ILLUMINATION PATTERN AND MATERIAL PROPERTIES

Irregular deviations from the shape of the mirror described by Eq. (1) may cause deterioration of the optical properties of the mirror. We start from the discussion of effects of shape imperfections of various scales and then relate them to requirements to the heating beam and the uniformity of material properties.

We concentrate on deviation causing tilts of the surface in the "long" directions, as those deviations produce the strongest deflection of the beam. The tilts in the "short" directions are much more forgiving. An angle that the mirror surface forms with a horizontal surface in some characteristic point z_1 (Fig. 2), halfway between the center and the ridge, is

$$\varphi \sim 1/f. \tag{41}$$

The deviation from this angle by some small amount $\delta\varphi$ would lead to a displacement of the beamlet reflected from the corresponding point of the mirror by the distance

$$\delta r \sim F\delta\varphi \tag{42}$$

Assume that we want the beam radius r_F in the focus be C times less than the initial beam radius,

$$r_F = \frac{r}{C} \tag{43}$$

Taking δr be $r_F/3$ (to provide sufficient margin with respect to the associated broadening of the focal spot), we obtain the following relation for the admissible level of deviations from the shape (1):

$$\delta\varphi = \frac{r_F}{3F} = \frac{1}{6Cf} \tag{44}$$

Non-uniformities of the incident radiation can be characterized by the lengh-scale l of the variation of the fluence across the heating area. For the length-scale l, the admissible amplitude h_l of deviations from the "perfect" relief (1) is

$$h_l \sim l\delta\varphi \sim \frac{l}{6Cf} \tag{45}$$

In other words, the constraint on the admissible surface "waviness" is most severe for the small-scale perturbations. The characteristic height of the "rim" is presented by Eq. (36). Relating the estimate (45) to it, one finds:

$$\frac{h_l}{h_{\max}} \sim \frac{2l\theta}{3Cr} \tag{46}$$

Now we relate Eq. (46) to the estimates of admissible non-uniformities in the auxiliary laser beam. As the height of the bumps is directly related to the non-uniformity of the fluence (by virtue of Eq. (26)), one can immediately state that the relative amplitude ε of non-uniformities in the fluence must be small enough:

$$\varepsilon < \frac{2l\theta}{3Cr} \tag{47}$$

For the perturbations of the largest scale (comparable to the long axis of the beam imprint, $l \sim 2r/\theta$, the admissible relative amplitude ε is $\varepsilon \sim 4/3C$. Assuming that $C=10$, one finds that the admissible relative variations of the fluence over the large scale are more than 10% - a condition which is easy to satisfy. For smaller-scale non-uniformities, less than, roughly, 1/15 of the length of the mirror, the admissible level becomes less than 1%, something that may require a careful design of the auxiliary laser, including possible use of random-phase plates [14, 15]. Non-uniformities of even smaller scale would be eliminated, most probably, by a combined effect of random phase-plates and lateral heat transport (which will smooth perturbations of the scale less than half of the beam radius).

A more serious issue could be non-uniformity of the absorbing properties of the surface (for the light of the auxiliary laser): the relative variation of the absorption coefficient must satisfy Eq. (47). This may be a challenging task.

Finally, for a "perfect" irradiation pattern and uniform albedo, the waviness can be created by the non-uniformity of the material properties, namely by non-uniformities of the parameter $\alpha(1+\mu)/c_p$, Eq.(26). If the slab is a polycrystal, one might be concerned with non-uniformities at the scale of crystallites. If, however, the size of those is small compared to the heat penetration depth, an averaging over large ensembles would occur, substantially reducing possible non-uniformities. Making the mirror of the material of the type of amorphous metals may be another approach. The larger-scale non-uniformities, at the scale ~ the beam radius and more, should be controlled at the manufacturing stage of the slab.

VIII. DIFFRACTION LIMITATIONS

The diffraction broadening of the beam in the focal plane can be evaluated as:

$$\delta\theta \sim \frac{\lambda}{2r} \tag{48}$$

If one wants to have the radius of the focal spot to be C times smaller than the initial radius of the beam, one has to impose a constraint $F\delta\theta < r/(3C)$ (we have introduced an additional factor of 3 as a safety margin). In other words, the following constraint must hold:

$$F < \frac{2r^2}{3\lambda C} \tag{49}$$

Combining this result with Eq. (33), one obtains the following relation between r and θ:

$$r\theta > \frac{3\sqrt{2\pi}q\lambda C}{8(1-\mu^2)}\frac{E}{G} \tag{50}$$

The role of this constraint is illustrated on Fig. 8. One sees that it is satisfied for angles θ compatible with the sufficient reflectivity (Table II) for 800 eV beam. However, it limits the possible focusing of the 8-keV beam.

The intensity increase in the focal plane compared to that of the un-focussed beam is, obviously, equal to

$$N = C^2 A_x(\theta) \tag{51}$$

For a given N, the condition (50) written in the equality form determines the curve of N=const in the (r, θ) plane. Using the data on $A_x(\theta)$ from Ref. 5, one finds the curves presented on Fig. 9.

IX. ENERGY OF THE AUXILIARY PULSE.

The thermal energy required to create the desired relief can be evaluated from Eq. (26). Integrating Q over the aperture of the x-ray beam, one easily obtains that the absorbed energy should be

$$W_b = \frac{3\pi}{16}\frac{r^4 c_P}{F\theta^2\alpha(1+\mu)} \tag{52}$$

where the subscript "b" refers to the aperture of the beam. As has already been mentioned, in reality, a broader area should be heated. Details depend on the intensity distribution in the wings of the auxiliary beam. We will take this factor into account just by multiplying Eq. (52) by 4. We have also to take into account that the albedo A_a of the mirror for the auxiliary beam is different from zero. Therefore, the energy of the heating pulse has to be multiplied by $(1\text{-}A_a)^{-1}$. Collecting all these factors together, we find that the total energy of the heating pulse should be

$$W = \frac{3\pi r^4 c_P}{4F\theta^2\alpha(1+\mu)(1-A_a)} \tag{53}$$

Using Eq. (38), one can obtain an alternative representation (assuming that we are working in the regime that provides the shortest focal length):

$$W = 3\sqrt{\frac{\pi}{2}} \times \frac{c_P(1-\mu)r^3}{\theta q\alpha(1-A_a)} \times \frac{G}{E} \tag{54}$$

This energy W is presented in Table IV and ranges between 30 mJ and 2 J. The average power of the auxiliary system $<P>$ is, obviously, W/t_x, where t_x is the time interval between two successive x-ray pulses. The numbers presented in Table IV correspond to $1/t_x$=120Hz. One sees that $<P>$ ranges from ~4 W to ~ 200 W.

An important parameter of the heating system is the energy flux P (energy per unit surface area per unit time). It can be presented as:

$$I = \frac{4}{1-A_a} \times \frac{Q}{t_0} \tag{55}$$

We introduced here a margin of 4, to take into account that the power, for the optimum pulse shape has a maximum which is a few times higher than Q/t_0. Note also that I contains a factor of $1/(1-A_a)$ that accounts for the albedo of the auxiliary beam. The power flux has a maximum at the "rim" of the mirror, where h is determined by Eq. (36). Using Eqs. (26) and (34), one finds:

$$I_{\max} = \frac{24c_P\chi}{\alpha(1-A_a)(1+\mu)F\theta} \tag{56}$$

For the smallest possible focal length determined by Eq. (38), one finds:

$$I_{\max} = \frac{96c_P\chi(1-\mu)}{\sqrt{2\pi}Sr\alpha(1-A_a)} \times \frac{G}{E} \tag{57}$$

Assuming that A_a=0.5, and S=1.5, and taking the other parameters from Table II, we find that required energy fluxes are very modest, Fig. 7. The duration of the heating pulse is also shown in Fig. 7. The energy flux I_{max} is several orders of magnitude lower than the surface flash-over limit, so that the heating will occur in a benign manner.

The required illumination pattern can be obtained by using a single non-axisymmetric lense that will convert, say, a gaussian axially-symmetric beam to the beam of a strongly-elongated cross-section. The intensity distribution on the surface of the metal slab would also be controlled by this lense. An advantage of this approach is that it will allow reaching a high accuracy of the intensity distribution. A disadvantage is that it does not allow changing the illumination pattern from pulse to pulse (a set of several lenses can be made to alleviate this problem).

The other solution could be the use of numerous beamlets with an independent intensity control. The radius of each beamlet should be such that the heat diffusion time over this size be much less than the total duration of the auxiliary pulse. This would cause a rapid smoothing of the temperature distribution on small scales and create a smooth average pattern which can be controlled even on a pulse-to-pulse basis. These beamlets, in fact, should not necessarily have circular cross-section. They can be made strongly elongated in the “long” direction, whereas the smoothing would occur in the “short” direction. Approximately 100 beamlets would then be sufficient to cover the whole mirror.

X. SHIFTING THE REFLECTING SURFACE

After the passage of the main pulse (which adds very little to the overall absorbed energy – the damage is caused because its energy is deposited in a very narrow surface layer), one needs to shift the slab so that, in the next pulse, a pristine surface is exposed.

To reduce the velocity at which the shift occurs, one should move the slab in the direction of the minor axis of the ellipse (Fig. 1). The distance must be large-enough, so that the heat from the previous pulse would not distort the new surface element. At the repetition rate of $1/t_x$=120 Hz (the t_x is the period of x-ray pulses), the heat between two pulses will diffuse by the distance

$$s \sim \sqrt{2\chi t_x} \sim 1 \text{ mm}. \tag{58}$$

We assume that the slab thickness is greater than 1 mm. The length of the heated zone, $2r/\theta \sim 1$ cm, will remain unchanged. Therefore, according to Eq. (26), the residual distortion of the surface will be of order

$$\frac{\delta h}{h} \sim \frac{r}{s} \tag{59}$$

Even for a small-size beam with r= 60 μm, the relative distortion is pretty large, ~ 6%, and 5 times higher for the larger-radius beam. Accordingly, the new spot has to be moved by a distance ~ 3s~3 mm from the old spot, in order to reach a surface not distorted by the previous pulse. This then yields the following expression for the velocity at which the slab has to be moved :

$$\mathrm{v} \sim 3\frac{s}{t_x} \sim 3\sqrt{\frac{2\chi}{t_x}} \tag{60}$$

This velocity for aluminum and beryllium is, roughly, 40-50 cm/s, i.e., rather trivial. Rotating disk or a rotating cylinder can be a solution (Fig. 3). To provide a larger surface

area, the disk or cylinder should also be slowly moved in the directions shown by block arrows on Fig. 3.

For the auxiliary pulse-length determined by Eq. (34), displacement of the surface in the *y* direction during the auxiliary pulse is

$$\frac{\delta y}{r} = \frac{v t_0}{r} = \frac{3\sqrt{2}}{8}\sqrt{\frac{r^2}{t_x \chi}} \qquad (61)$$

In the thermo-elastic analysis, we assumed that the surface is at rest with respect to the auxiliary beam imprint. In order this assumption to be valid, δy must be several times smaller than r. Imposing a factor of 5 as a safety margin ($\delta y < r/5$), one finds from Eq. (61) the following constraint:

$$\frac{1}{t_x} < 0.14\frac{\chi}{r^2} \qquad (62)$$

For the beam radius of 300 μm, this constraint limits the repetition rate to the value of ~ 100 Hz. If this is of an issue, one can fold the surface motion into the general thermo-elastic problem and make the corresponding corrections to the illumination pattern. For smaller beam radii, the condition (62) is easily satisfied (for the LCLS repetition rate).

One more related problem is that of an average heating of the disk. In a steady state, a strip will be formed on the surface of the disk, with the temperature exceeding the ambient temperature. This would produce some static distortion of the disk surface. Within one revolution the temperature must drop to an acceptable level by thermal conduction to other (perhaps, actively cooled parts), or by thermal radiation from the surface. Without discussing any specific solutions to this problem, we just note that it may be non-trivial in the case of large beam radius, where the average heating power

from the auxiliary laser can reach 100 W. Handling this problem will determine the disk dimensions.

XI. VARIATIONS OF THE SYSTEM

In this section, we briefly describe several possible variations of this general approach.

1. One can use an initially non-planar surface to achieve better focusing. This will be a 1D non-planarity, easy to manufacture. An example of this is shown on Fig. 3 c. Reflections would occur from the inner surface of the cylindrical shell, so that the focusing in the direction perpendicular to the surface will occur even without any auxiliary heating. One can then heat the inner surface of the cylinder in such a way, that the heated patch is substantially broader than the x-ray beam radius and has a length in the direction of the long axis of the beam imprint somewhat greater than the length of the imprint. By that one creates conditions where the penetration depth of the heat may substantially exceed a third of the beam radius, as was assumed in Sec. IV. This, in turn, leads to the possibility of increasing the curvature in the direction of the major axis and thereby reducing the focal length.

2. Along the same line, one can focus the beam in only one direction (cylindrical mirror), in the direction y on Fig. 1. This would yield a substantial intensity increase in the focal plane, although the focus now will be a line. Incidentally, for the 0.8 keV beam, where the radius of curvature of the mirror is rather large, one can use this technique even without resorting to the TEL concept, just by making a cylindrical mirror as shown on Fig. 3c.

3. One can conceive of using, as an auxiliary heating source, a 30-50 keV electron beam, instead of a laser. An advantage is a large penetration length of such beams. Therefore, one would not have to wait for the heat to propagate over the distance of, say, 100 μm (as was the case of a 0.8 keV beam): the required profile can be created within the time of order of a few sound propagation times, which is of order of a microsecond even for large optics (1 mm radius). This, on the one hand, would allow one to substantially increase the repetition rate and, on the other hand, to reduce the heating power (because of a very low albedo of electron beams). A disadvantage is that this technique could hardly be used for dielectric surfaces.

4. Finally, when one considers a large-scale optics, of the size of a few millimeters to a few centimeters, one can switch to the use of slabs with a thickness *a* a few times less than the optics radius (Fig. 10). As is well known [12], in this case large deformations are possible for small stresses. This allows one to substantially reduce the *f*-number compared to that achievable for thick slabs.

We present here (without derivation) equations analogous to Eq. (24) and (27):

$$\frac{\partial^2 u_x}{\partial y^2} = -\frac{4\alpha(1+\mu)}{a^3}\int_0^a \left(x' - \frac{a}{2}\right)\delta T(x', y)dx'; \qquad (63)$$

$$\sigma_{yy} = \frac{\alpha E}{3(1-\mu)a}\left[-\delta T + \frac{1}{a}\int_0^a \delta T(x', y)dx' + \frac{12}{a^3}\left(x - \frac{a}{2}\right)\int_0^a \left(x' - \frac{a}{2}\right)\delta T(x', y)dx'\right] \qquad (64)$$

This result corresponds to a 2D problem, where the dependence of all parameters over the coordinate *z* is suppressed. The other components of the stress tensor are negligibly small (in the case of a thin slab). Equations (63)-(64) show that, for the size of the heating zone comparable with the beam radius *r*, one can reach the same focal length as for a thick

slab, at a stress level smaller by a factor of $(a/r)^2$. This allows one to reduce the *f*-number of the mirror accordingly. An obvious difficulty in applying a thin-slab approach to the LCLS optics is a small beam radius. On the other hand, this approach should be quite helpful for the larger-size optic.

XII. DISCUSSION

We believe that we have demonstrated the feasibility of creating transient renewable optics by providing a proper spatial and temporal heating pattern of the surface of an initially planar slab of a reflecting material.

The concept is realizable for the whole range of LCLS beam energies (0.8-8 keV). For the energies below 2-3 keV, the intensity of the focal plane can be increased by a factor N=100-150 compared to an un-focused x-ray beam. Incidence angles are in the range 10 – 30 mrad.

Most challenging problem is focusing a 60-μm radius, 8-keV beam: the incidence angle should be very shallow, to ensure a high reflectivity. The shallowness of the incidence angle imposes severe constraints on the accuracy of the alignment and the quality of the surface and, in addition, leads to a large focal length and early onset of diffraction limitations. Still, even in this most challenging case, one can increase the intensity by a factor of N=10 compared to the un-focused beam.

An attractive feature of the TEL optics is the possibility to change the shape of the mirror from pulse to pulse, without any mechanical contact with the reflecting surface.

Although the primary motivation for this study were potential needs of the LCLS facility, the results presented are of a broader applicability. The possibility of creating a focusing mirror on any reflecting surface, without making any direct contact with the surface,

may be of interest for applications involving pulsed main beams with the wavelengths from optical to x-ray range. This can prove to be less expensive than even creating a fine permanent optics for low-intensity pulsed beams, especially if the change of the focal length and direction of the radiation may be needed in the course of work. In such cases, our analysis can serve as a template for designing such optics, as the issues of thermal stresses, required surface quality, diffraction limitations, auxiliary heating system, etc, can be assessed on the basis of the general equations provided in this paper.

Acknowledgment

I am grateful to A. Toor and A. Wootton for supporting my participation in the LCLS project in 2000-2002. This work was performed under the auspices of the U.S. Department of Energy by University of California Lawrence Livermore National Laboratory under contract No. W-7405-Eng-48.

References.

1. The LCLS Design Study Group. *Linac Coherent Light Source (LCLS) Design Study Report* , Report SLAC-R-521, Stanford University, 1998.
2. T. Tschentscher. *"XFEL laboratory at TESLA."* In: Proceedings of SPIE (R.O. Tatchyn, A.K. Freund, T. Matsushita – Eds), v. 4500, p. 1 (2001).
3. *LCLS - The first experiments. Report of the Scientific Advisory Committee for the Linac Coherent Light Source,* September 2000.
4. A. Wootton, J. Arthur, T.Barbee, R.Bionta, A.Jankowski, R. London, D. Ryutov, R. Shepherd , V. Shlyaptsev, R.Tatchyn, A.Toor. Nuclear Instruments & Methods in Physics Research Section A-Accelerators Spectrometers Detectors & Associated Equipment. **483**, 345, 2002.
5. B.L. Henke, E.M. Gullikson , J.C. Davis. Atomic Data and Nuclear Data Tables, **54**, 181 (1993).
6. R.A. London, R.M. Bionta, R.O. Tatchyn, S. Roesler. *"Computational Simulations of High-Intensity X-Ray Matter Interaction."* In: Proceedings of SPIE (R.O. Tatchyn, A.K. Freund, T. Matsushita – Eds), v. 4500, p. 51 (2001).
7. D.D. Ryutov. Rev. Sci. Instr., **74**, 3722 (2003).
8. J. Kuba, A. Wootton, R.M. Bionta, et al. Nuclear Instruments & Methods in Physics Research Section A-Accelerators Spectrometers Detectors & Associated Equipment. **507**, 475 (2003).
9. D.D. Ryutov. *Multi-pulse effects in the damage to the LCLS reflective optics.* To be published in Proc. of the 49th Annual SPIE Meeting, Denver, CO (2004).
10. D. Ryutov, A. Toor. Rev. Sci. Instr., **72**, 4042 (2001).
11. D. Ryutov, A. Toor. *"Renewable liquid optics with magneto-electrostatic control."* In: Optics for Fourth-Generation X-Ray Sources, Proceedings of SPIE, v. 4500, p. 140 (2001).
12. L.D. Landau and E.M.Lifshitz. *Theory of Elasticity* (NY, Pergamon Press, 1986).
13. L.D. Landau and E.M.Lifshitz. *Fluid Mechanics* (NY, Pergamon Press, 1987).
14. R.H. Lehmberg, S.P. Obenshain. Opt. Commun. **46**, 27 (1983).
15. Y. Kato, K. Mima, N. Miyanaga, S.Arinaga, Y. Kitagawa, M. Nakatsuka, C. Yamanaka. Phys. Rev. Lett., **53**, 1057 (1984).

Table 1. Parameters of the x-ray beams in the experimental hall nearest to the undulator

Photon energy, keV	Beam radius μm	Pulse duration, fs	Rep-rate, Hz	The number of photons per pulse	Fluence per pulse, J/cm^2
8 (λ=1.8 Å)	60	260	120	$2\cdot10^{12}$	23
0.8 (λ=18 Å)	300	260	120	$2.2\cdot10^{13}$	1

TABLE II. Reflectivity for an initially unpolarized light [5]

		θ=1/300 rad		θ=1/100 rad		θ=1/30 rad		θ=1/10 rad	
		σ = 0	σ = 5	σ = 0	σ = 5	σ = 0	σ = 5	σ = 0	σ = 5
Ag	E=0.8	0.95	0.84	0.85	0.59	0.55	0.15	0.028	0
	E=8.0	0.92	0.74	0.05	0	0	0	0	0
Al	E=0.8	0.98	0.97	0.95	0.92	0.75	0.62	0.002	0
	E=8.0	0.95	0.92	0.002	0	0	0	0	0
Be	E=0.8	0.99	0.99	0.97	0.96	0.6	0.47	0	0
	E=8.0	0.48	0.33	0	0	0	0	0	0

Notation: E – x-ray energy, keV; θ - incidence angle (measured from the surface of the mirror) in radians; σ – surface roughness, nm. If the reflectivity is below 10^{-3}, we put 0 in the corresponding box. Shown in red are reflectivities that are acceptable/marginally acceptable.

TABLE III Some thermo-mechanical parameters of aluminum and beryllium

Parameter	Notation and units	Magnitude	
		Al	Be
Volumetric thermal expansion coefficient, $\Delta V/V=\alpha\Delta T$	α, 1/K	$6.9\cdot10^{-5}$	$3.15\cdot10^{-5}$
Young modulus	E, n/m^2	$6.9\cdot10^{10}$	$30\cdot10^{10}$
Yield strength*	G, n/m^2	$30\cdot10^{7}$	$150\cdot10^{7}$
Poisson ratio	μ	0.37	0.2
Longitudinal sound speed	$s_{\|\|}$, km/s	6	12.5
Transverse sound speed	$s_{\perp}$, km/s	3	8.8
Density	ρ, g/cm^2	2.7	1.85
Thermal capacity	c_p, J/(cm$^3\cdot$°K)	2.5	3.3
Thermal diffusivity	χ, cm^2/s	0.87	0.52
Temperature increase per pulse, Eq. (29), for S=1.5	$\delta T^* K$	80	250
Melting temperature	T_m, K	930	1560

* The number for aluminum corresponds to an aluminum alloy with 2.2 % of copper and 0.2-0.5 % of chromium.

TABLE IV The energy of the auxiliary pulse and average power at 120 Hz

	W, Joules/<P>, Watts	
	8-keV beam (r=60 μm, θ=3 mrad)	0.8-keV beam (r=300 μm θ=30 mrad))
Al	0.036/4.3	0.445/53.4
Be	0.153/16.4	1.92/230

The average power is defined as the energy per pulse W divided by the time between pulses, t_x. The numbers in the table correspond to the LCLS rep-rate: $1/t_x$=120 Hz.

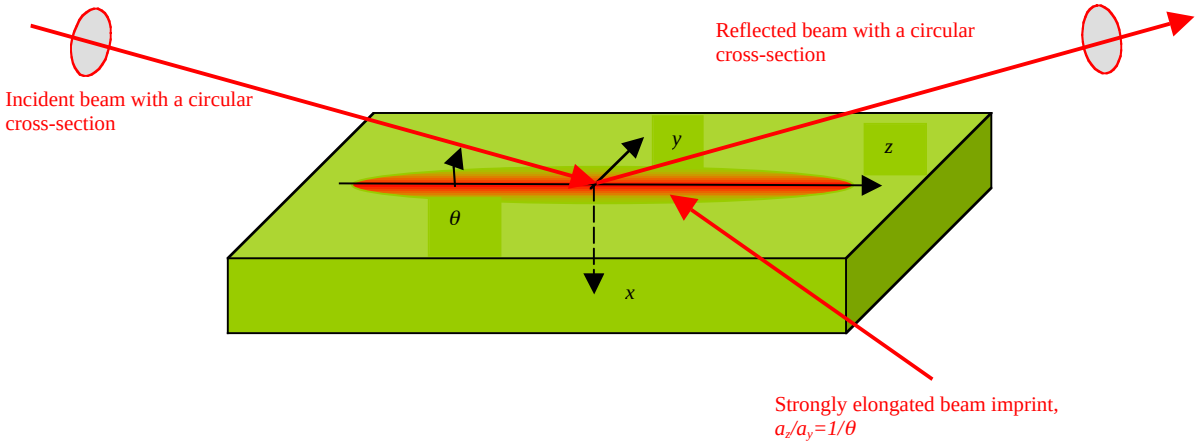

Fig. 1 Grazing-incidence reflection of the x-ray beam from the planar surface. The beam Imprint on the surface is shown as an elongated elipse. Note the orientation of the axis x: for this orientation, the surface displacement towards the vacuum side, u_x, is negative. In the "optical" part of this report we use notation $h \equiv -u_x$.

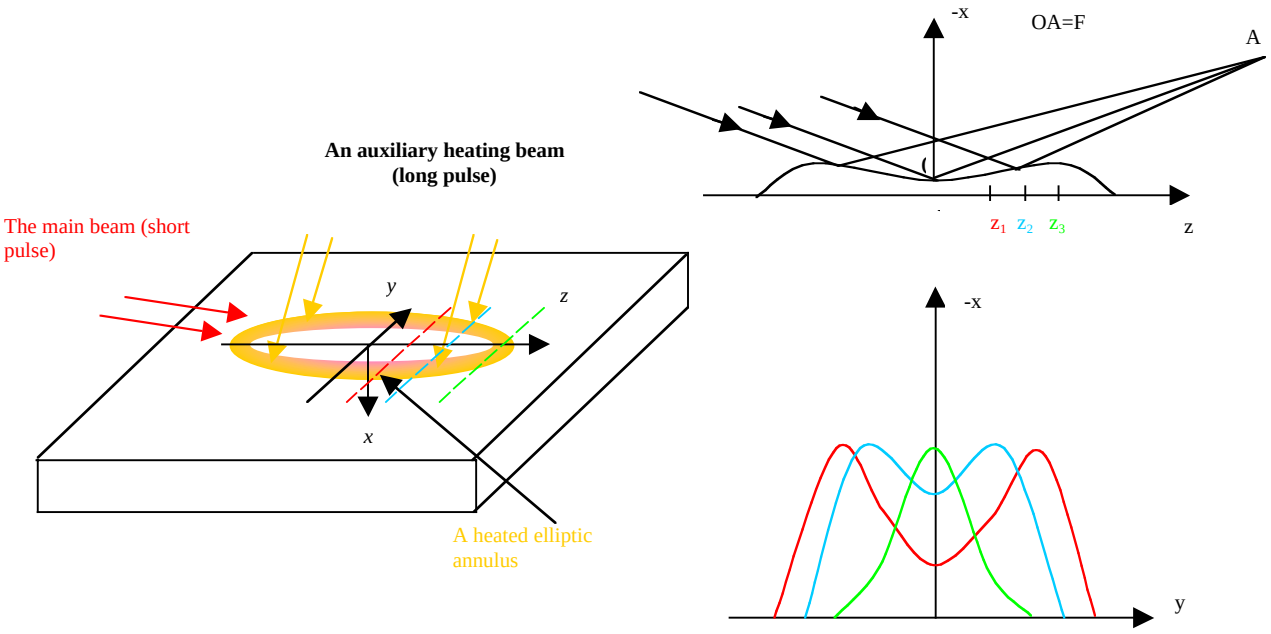

Fig. 2 The principle of the TEL optics: an auxiliary pulse (yellow) heats the surface prior to arrival of the main pulse (red). The heat distribution is chosen so as to create (via thermal expansion) an elliptic mirror. The upper-right panel shows the surface profile along the long axis of the imprint; the lower-right panel shows the profiles along dashed lines on the left panel.

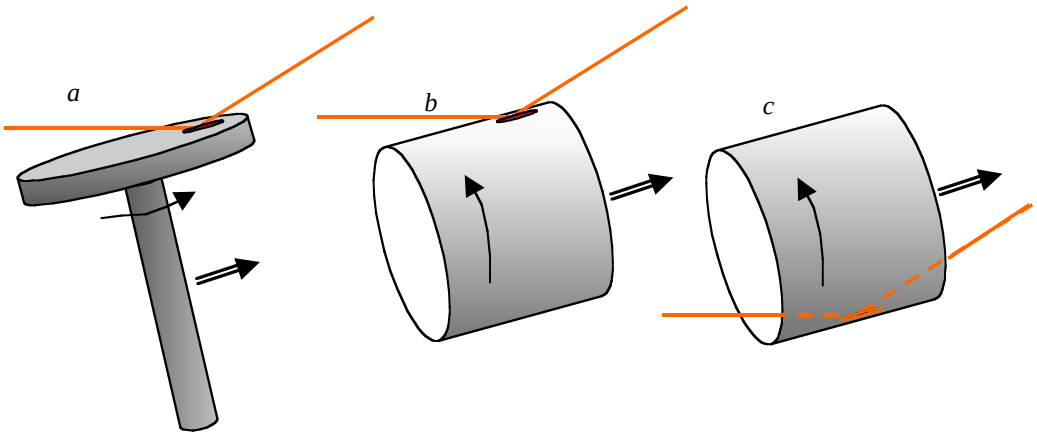

Fig. 3 Possible ways of providing the “fresh” surface for every x-ray pulse. In the case of a cylinder, its radius should be substantially greater than the radius of curvature of the elliptic mirror in the “short” direction, which is typically 1-2 cm. The block arrows show the direction of a slow motion required for a complete coverage of the whole surface of a disk (cylinder).

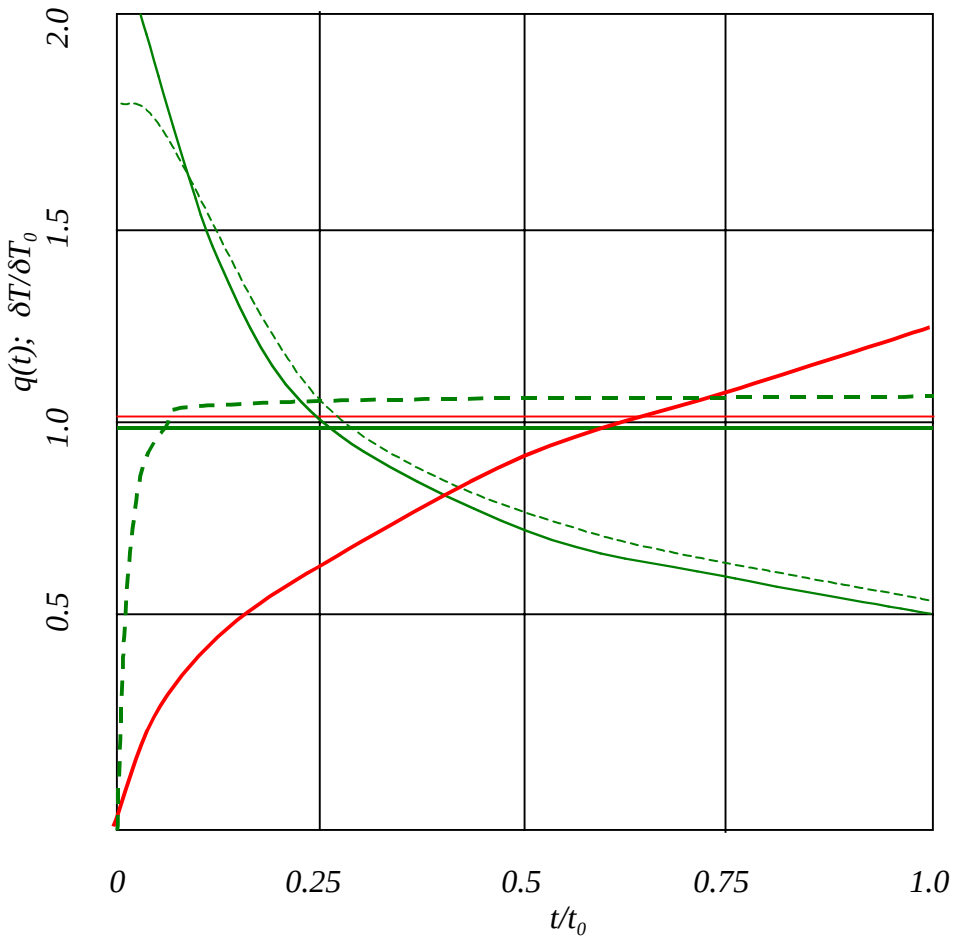

Fig. 4. Heating of the slab. Green lines correspond to an optimum (solid lines) or near-optimum (dashed lines) pulse shape. Thin lines represent *q(t)*, thick lines represent normalized surface temperature. The *q* shape represented by the dashed line removes a singularity near $t=0$. Thin red line represents the constant heating power, $q=1$; thick red line represents the corresponding surface temperature.

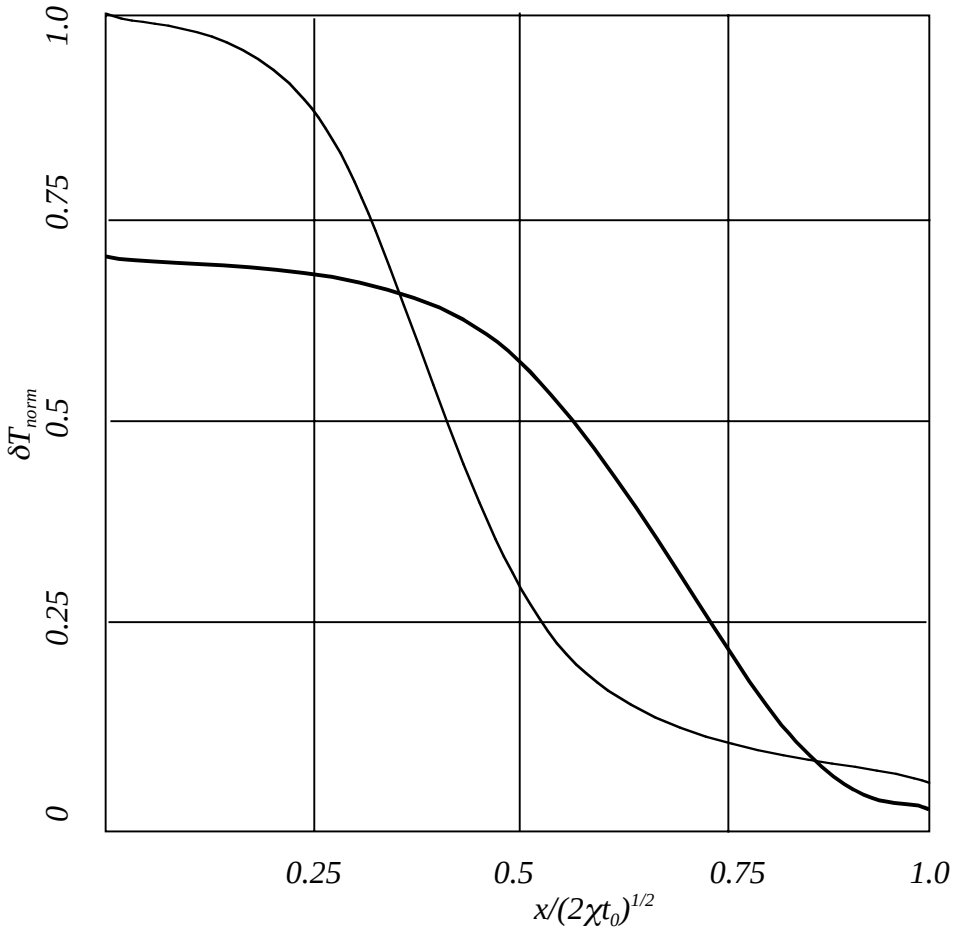

Fig. 5 Temperature distributions over the thickness of the plate at the end of the heating pulse normalized to the surface temperature at that instance for the flat-top heating. Thin line corresponds to the flat-top heating profile, whereas thick line corresponds to the optimum heating profile. The total heat delivered per unit surface area is the same. Note that the surface temperature in the optimum case is smaller, and the profile is broader.

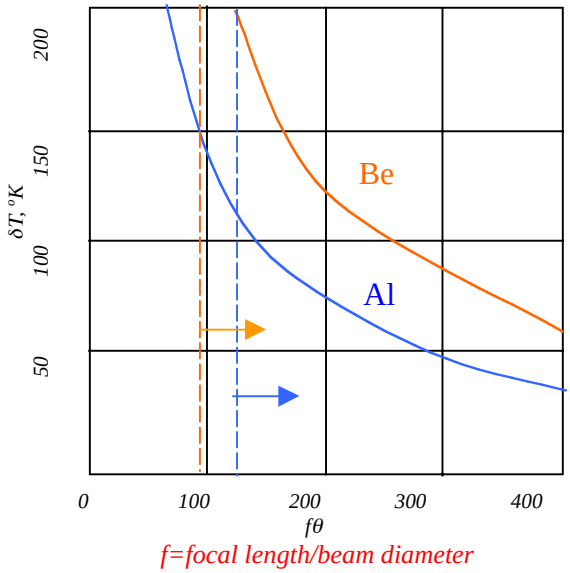

Fig. 6 The required temperature increase vs the $f\theta$ product.

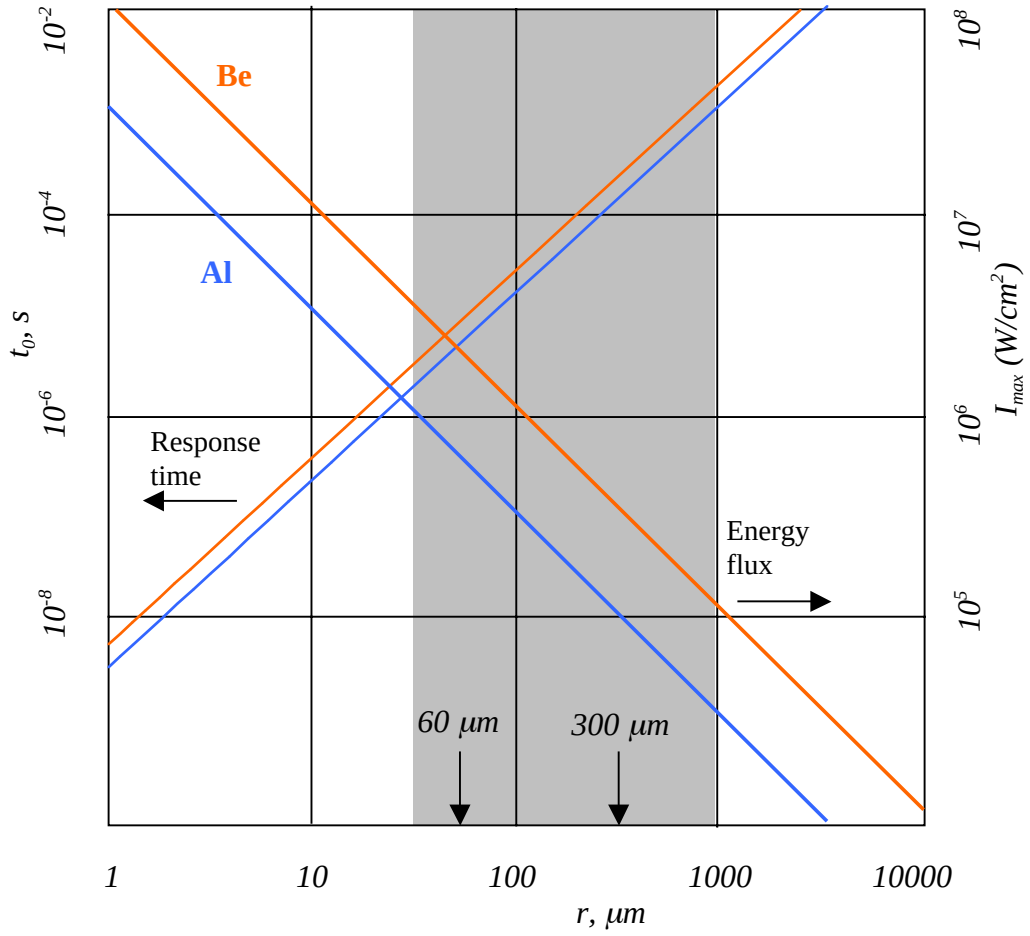

Fig. 7. Response time (Eq. (34)) and auxiliary heating energy flux (Eq. (57)) for aluminum (blue) and beryllium (orange) vs. the beam radius. Thin lines (left scale) represent response time, thick lines (right scale) represent energy flux. The shaded area corresponds to the x-ray beam radii between 30 μm and 1 mm, where the TEL approach seems most promising.

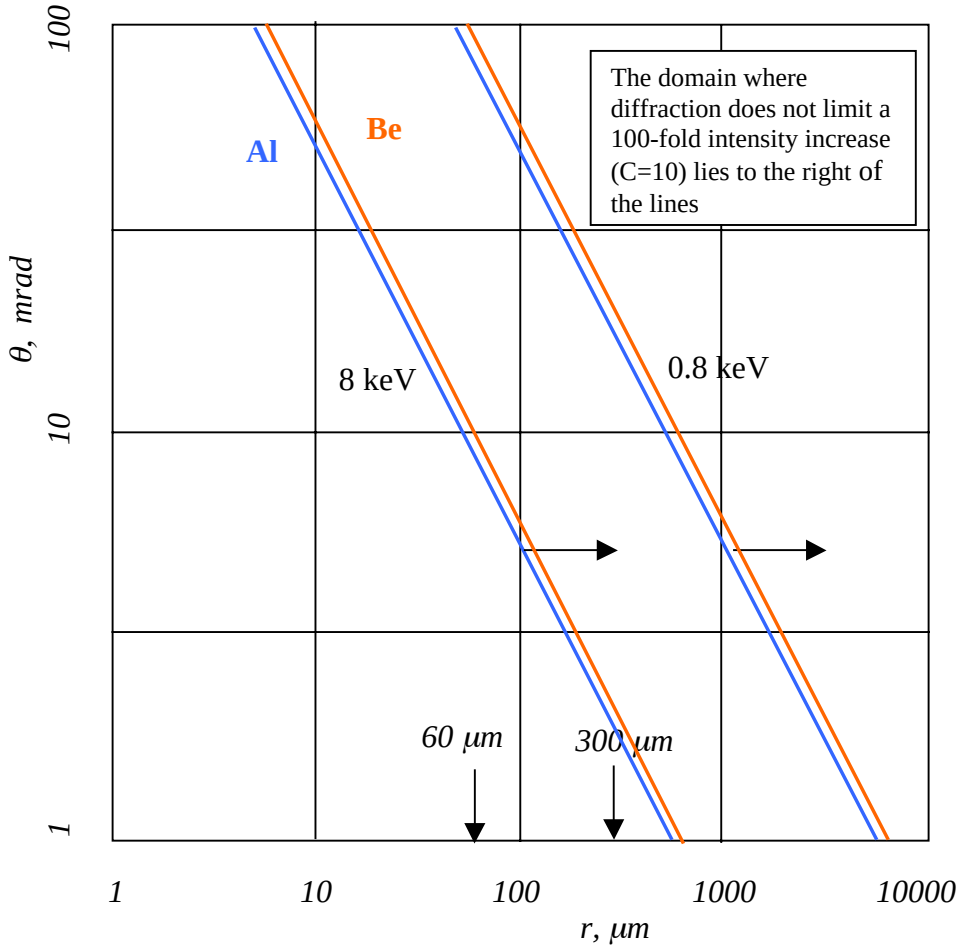

Fig. 8. Diffraction limitations. To the right of these curves a 100-fold intensity increase is possible. Note that the 8-keV beam at θ=3 mrad determined by the requirement of a high-enough reflectivity, does not satisfy this criterion. A more detailed analysis shows that only 10-20 –fold increase is possible for this beam (depending on the mirror material).

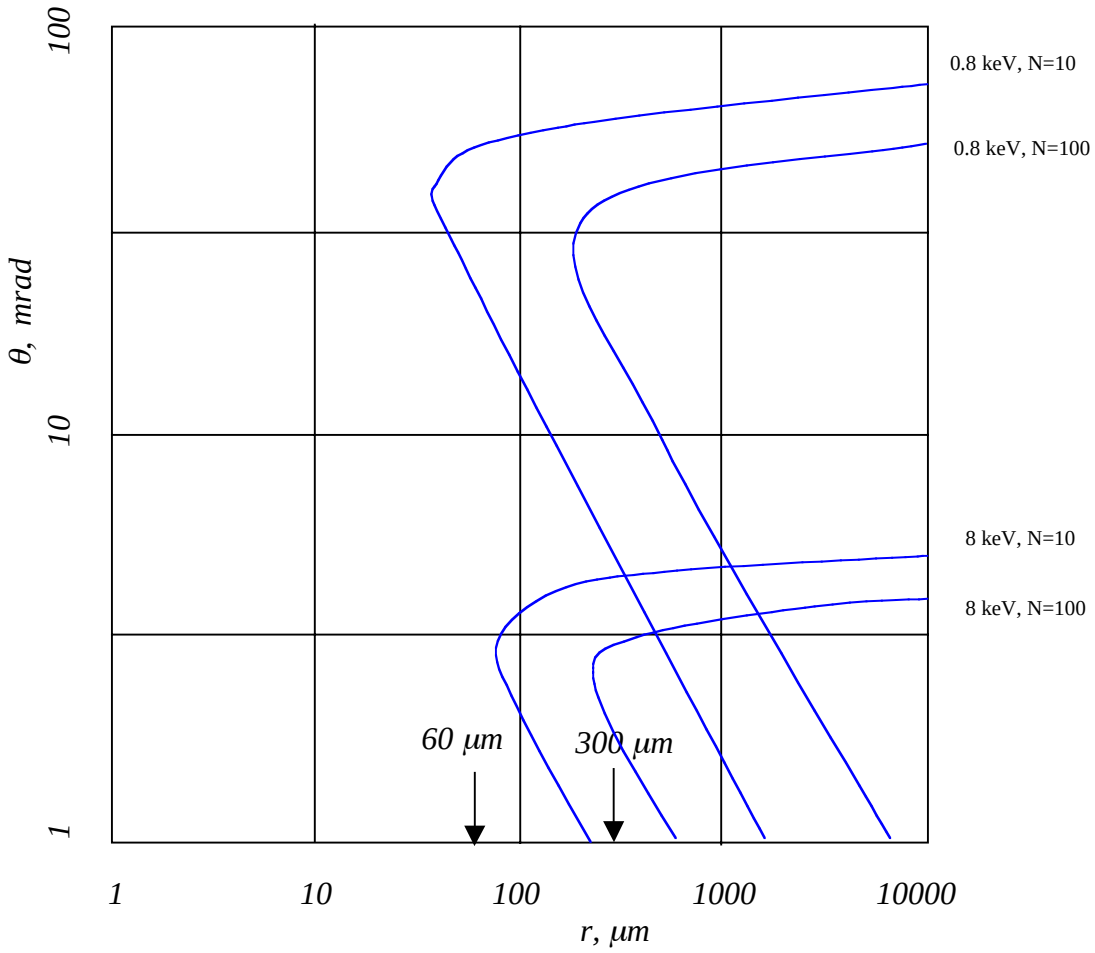

Fig. 9 Isolines of the parameter N for aluminum reflector.

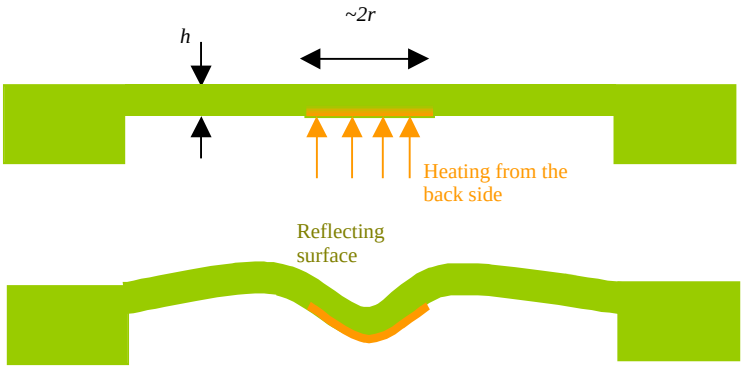

Fig. 10. Creating a mirror of the slab with a thickness less than the beam radius. The heating from the back side becomes possible, and constraints on the achievable focal lengths become less severe. Can work for larger-scale optics (r>1 mm).